

# Spill-over process of hydrogen sorption on palladized alumina, yttria and zeolite 4A

M. V. ŠUŠIĆ

Faculty of Physical Chemistry, University of Belgrade, PO Box 550, YU-11001 Belgrade, Yugoslavia

Doping of alumina, yttria and zeolite 4A with small quantities of palladium (down to 0.025%) was done. It was shown that these oxides, which do not normally absorb hydrogen, after the doping acquire a considerable capacity for hydrogen absorption. The sorption of hydrogen is occurring by the spill-over effect from metallic palladium to the oxide. The process is exothermal, taking place in two stages between 60 and 350 °C. Activation energies of the first stage range from 120 to 167 kJ mol<sup>-1</sup> and for the second one from 20 to 30 kJ mol<sup>-1</sup>. After cooling to room temperature in hydrogen flow, the samples are able to absorb considerable quantities of oxygen which reacts exothermally with the previously formed hydride. On next exposition to hydrogen, a vigorous reaction of it with the adsorbed oxygen is taking place already at room temperature. Enthalpies of hydrogen absorption,  $-\Delta H$ , are of the order of 10 kJ g<sup>-1</sup>, showing a tendency of increase after repeated exposures to hydrogen.

## 1. Introduction

The oxide bronzes  $A_xMO_n$  belong to a class of ternary oxide phases which are formed by substitution of an electropositive element A in an  $MO_n$  matrix by a transition element M [1, 2]. Examples of oxides forming oxide bronzes of particular importance are  $WO_3$ ,  $MoO_3$ ,  $V_2O_5$  and other similar compounds. The significance of these oxides (bronzes) is their ability to acquire hydrogen forms such as  $H_xMO_3$ ,  $H_xWO_3$  etc. [3]. Hydrogen bronzes have been formed from hexagonal  $WO_3$  which absorbs hydrogen [4]. The presence of Pt or Pd considerably aids the formation of hydrogen bronzes [5, 6], involving the hydrogen spill-over process [7, 8]. With oxides containing small quantities of metallic palladium (less than 0.1%), the latter effects the transfer of molecular hydrogen first into the atomic form on palladium, wherefrom it "spills" into the oxide phase forming thus the hydrogen bronze. The presence of traces of Pd in the oxide enables, therefore, the oxide to absorb hydrogen. In some cases the hydrogen absorbed in the palladium-doped oxide phase may be transferred into Pd-free oxide, provided it is homogenized with the former. It has been shown [9] that with  $WO_3 + Pd$  and  $MoO_3 + Pd$  a reduction by hydrogen is taking place; subsequent oxidation by oxygen leads to a complex change in the structure of the sample. In the present work palladium-doped alumina, yttria and zeolite 4A are investigated along the same lines.

## 2. Experimental procedure

The preparation of  $Al_2O_3 + Pd$  and  $Y_2O_3 + Pd$  (both p.a. grade purity, Merck) was done by first

soaking them with an aqueous solution of  $Pd(NO_3)_2$  of known concentration. Such relatively dense dispersions were slowly dried with frequent mixing. They were further heated in air to 450 to 500 °C for 2 to 3 h. The palladium nitrate is under these conditions decomposed into metallic Pd which is uniformly dispersed on the solid oxide phase. The alumina sample prepared in such a way contained 0.6% of Pd, while the Pd content of yttria was 0.3%. All additions are in weight %.

By grinding of the above prepared alumina sample with an excess of Pd-free oxide in an agate mortar, a new sample containing an average 0.14% Pd was prepared.

Two samples of zeolite were also Pd-doped by mixing different quantities of powdered zeolite 4A (Union Carbide Co.) in the sodium form with Pd solutions of known concentrations and proceeding further as described above. One sample (I) contained 0.30% Pd and the other (II) 0.025%.

The kinetic and thermal parameters of the process of hydrogen absorption were determined by differential scanning calorimetry (DSC) by use of a Du Pont 1090 thermal analyser.

Kinetic examinations of the process were done by non-isothermal scanning calorimetry, as described in our previous articles [4, 9]. For first-order reactions it follows [10] that the rate constant is determined by the equation

$$k = \frac{\Delta mW}{A - a} \quad (1)$$

where  $\Delta mW$  is the ordinate value of the peak on the thermogram (in milliwatts) after a certain time  $t$  of absorption duration, i.e. at temperature  $T$ ;  $A$  is the

total area of the exo-peak, while  $a$  is the area of the exo-peak recorded up to time  $t$  of reaction duration. If the hydrogen absorption process is a first (or quasi-first) order reaction, it follows that a plot of  $\log k$  versus  $1/T$  should be linear. The slope should yield  $-E/R$ , i.e. the energy of activation, while the ordinate intercept is the logarithm of the frequency factor.

### 3. Results and discussion

#### 3.1. DSC investigations

##### 3.1.1. The $Al_2O_3 + 0.6\% Pd$ system

The DSC thermogram depicted in curve (a) of Fig. 1 shows that at programmed heating in a hydrogen flow, already at 50 to 60°C an exothermal process of hydrogen absorption begins, which is terminated at about 350°C; an expressed exo-peak is recorded. Analysis of the process kinetics by use of Equation 1 shows (Fig. 2) that broken straight lines are being produced, with two distinct slopes, yielding energies of activation of hydrogen absorption of two stages, i.e.  $E_1 = 120 \pm 20$  and  $E_2 = 19.8 \pm 0.2 \text{ kJ mol}^{-1}$ , respectively. The corresponding frequency factors are  $Z_1 = 6.2 \times 10^{15}$  and  $Z_2 = 33.1 \text{ s}^{-1}$ . Integration of the exo-peak yields the enthalpy of absorption of  $\Delta H = -11.4 \text{ kJ g}^{-1}$ .

After the first heating of the sample in hydrogen, it was cooled to room temperature still in a hydrogen atmosphere and later exposed to air for 30 min or longer. It was noted that the sample acquired a brownish colour during hydridation.

Following exposure of the sample to air (or oxygen), it was again heated in hydrogen flow, the hydrogen intake being begun at the moment of the heating start. From the moment of the first contact of hydrogen with the sample, a rapid and complex reaction starts, which produces the thermogram of curve (b) in Fig. 1. Due to the fast exothermal reaction, the sample heats itself faster than programmed by the equipment; the termination of the first stage is characterized by a loop, followed by sorption similar to the first heating of the sample. The almost explosive reaction of the first stage (which results in a scattering of the sample in the DSC cell) can be explained by a fast reaction of hydrogen with the oxygen of the oxide sample, being catalysed by the palladium that is present. Integration of the exo-peak yields the total enthalpy of the process as  $\Delta H = -14.4 \text{ kJ g}^{-1}$ , which is considerably greater (in the absolute sense) than the one in the first hydridation, shown in curve (a).

The fact that the sample after preparation and the first Pd-doping in air does not show such a violent reaction with hydrogen during the first hydrogen treatment means that the first hydridation changes the sorption properties of the sample (a reduction reaction which is reversible in the presence of atmospheric oxygen). The sample is now abundantly capable of absorbing oxygen from the air and reacts with hydrogen violently even at 10°C. The beginning of the recorded thermogram in curve (b) of Fig. 1, at a temperature of 36°C, is the moment of contact of

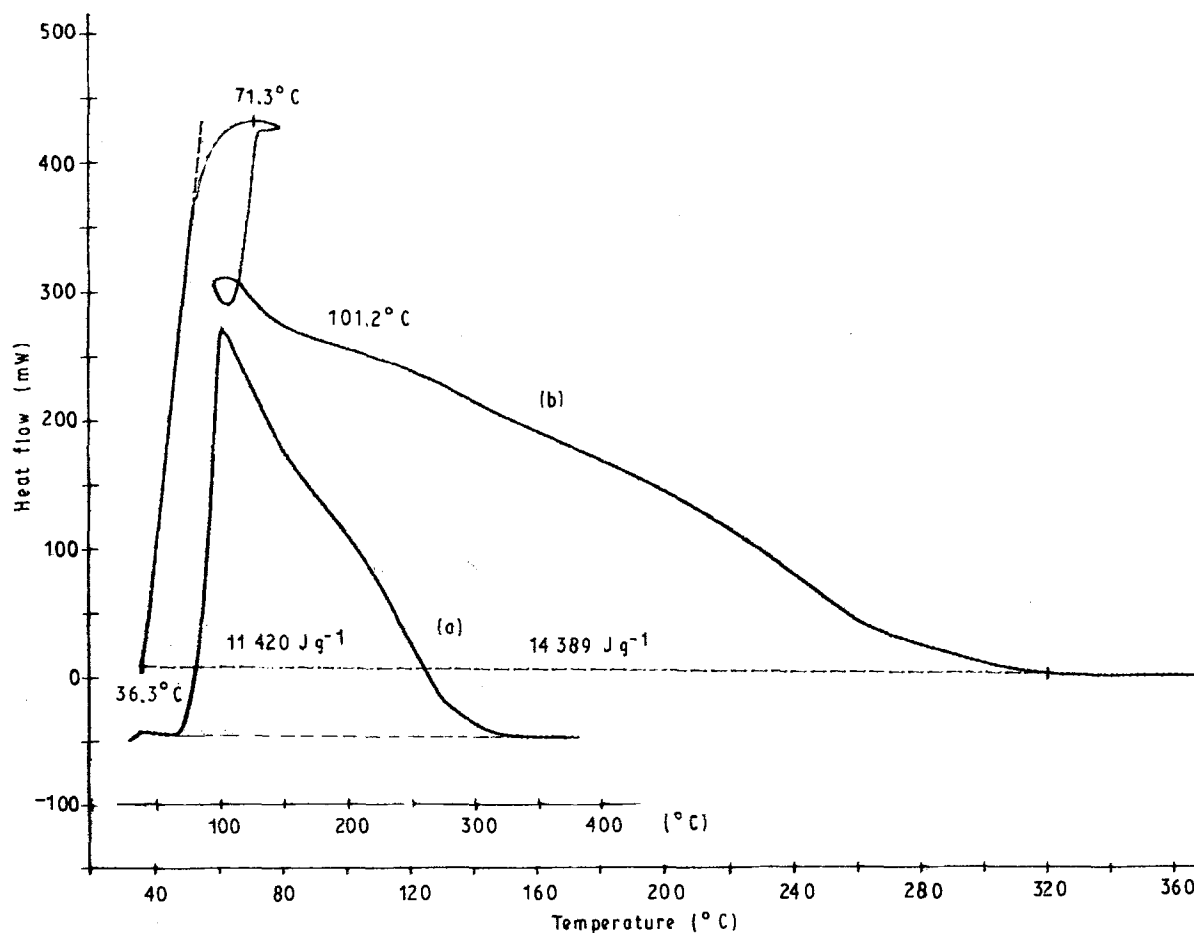


Figure 1 DSC thermograms of  $Al_2O_3 + 0.6\% Pd$  in hydrogen flow, heating rate  $30 \text{ K min}^{-1}$ : (a) first hydridation, (b) second hydridation after cooling in hydrogen and exposure to air for 30 min.

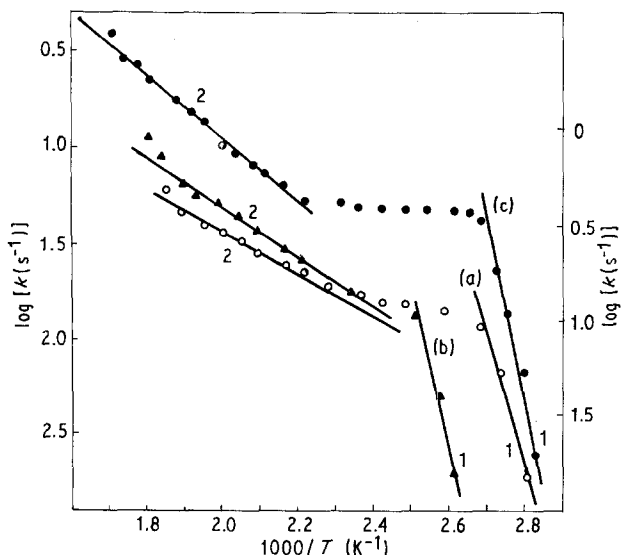


Figure 2 Activation energy plots of  $\log k$  versus  $1/T$ : (a)  $\text{Al}_2\text{O}_3 + \text{Pd-H}$ , (b)  $\text{Y}_2\text{O}_3 + \text{Pd-H}$  and (c) zeolite 4A + Pd-H.

hydrogen with the sample. It should be pointed out also that the increase of the enthalpy, following the reaction between hydrogen and oxygen, is due to the enlarged activation capacity of the spill-over effect of the palladium present; in the first hydridation it became considerably more dispersed and amorphized, an indication of which is the colour change.

### 3.1.2. The $\text{Al}_2\text{O}_3 + 0.14\% \text{Pd}$ system

The homogenized mixture of pure alumina and the palladized one with an average content of Pd of 0.14% shows that in the absorption process both components are taking part. The exo-peak in the DSC thermogram appears to be the same as in unmixed Pd-alumina. The kinetic analysis of the curve indicates that the mechanism of hydrogen absorption stays unchanged, despite the decreased concentration of palladium. The enthalpy of hydrogen absorption is the same, meaning that in the absorption the pure alumina is also taking part in the spill-over effect from palladized alumina.

### 3.1.3. The $\text{Y}_2\text{O}_3 + \text{Pd}$ system

This system behaves similarly to the one containing alumina with palladium. Curve (a) of Fig. 3 shows the DSC thermogram with the exo-peak corresponding to hydrogen absorption. From its shape it is obvious that the process proceeds in two stages. The kinetic analysis of data, shown in curve (b) of Fig. 2, produces again two sets of activation energies and frequency factors, i.e.  $E_1 = 157 \pm 25 \text{ kJ mol}^{-1}$ ,  $Z_1 = 9.5 \times 10^{19} \text{ s}^{-1}$  and  $E_2 = 24.4 \pm 0.3 \text{ kJ mol}^{-1}$ ,  $Z_2 = 130 \text{ s}^{-1}$ . The enthalpy was found after integrating over both maxima and for the first hydridation it amounts to  $\Delta H = -8.1 \text{ kJ g}^{-1}$ .

By comparison of curves (a) and (b) of Fig. 2, and Figs 1 and 3, one concludes readily that the hydrogen

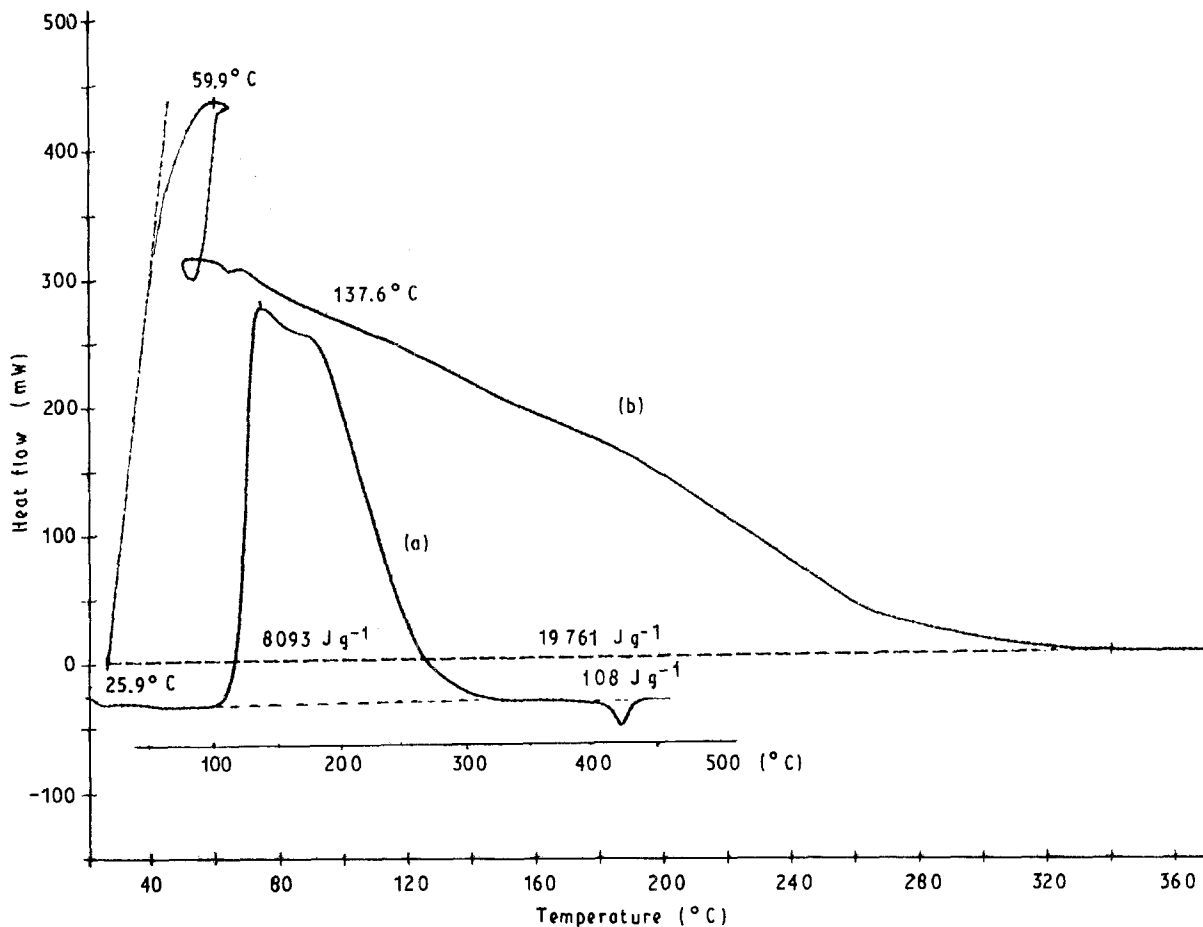


Figure 3 DSC thermograms of  $\text{Y}_2\text{O}_3 + 0.3\% \text{Pd}$  in hydrogen flow,  $25 \text{ K min}^{-1}$ : (a) first hydridation, (b) second hydridation after cooling in hydrogen and exposure to air for 30 min.

absorption takes place by the same mechanism in two stages with both palladized alumina and yttria. The first stages show larger activation energies and frequency factors. In the case of first hydridation of the  $Y_2O_3 + Pd$  system a small endo-peak appears at about  $420^\circ C$ , representing an irreversible endothermal process with  $\Delta H = 108 J g^{-1}$ , which could be due to some changes in the sample which were not further investigated by the thermogravimetric analysis (TGA) method. This effect is seen also in the case of the  $MoO_3 + Pd$  bronze at first hydridation [10].

As with the alumina + Pd system, the yttria + Pd system when cooled and exposed to air after hydridation undergoes oxygen absorption, producing again a violent reaction when exposed to hydrogen. Curve (b) of Fig. 3 shows a loop similar to that in curve (b) of Fig. 1. The effect is reproducible on repeated hydridations. The enthalpy of this process is larger than that of the first hydridation and is  $\Delta H = -13.8 kJ g^{-1}$ . The absorption capacity for hydrogen as well as for oxygen is increased after the first hydridation, as in the previous case.

### 3.1.4. The zeolite 4A system

As seen from Fig. 4, this system (sample I) behaves qualitatively in all respects like the above two systems. The two stages of the first hydridation proceed with  $E_1 = 167 \pm 28 kJ mol^{-1}$ ,  $Z_1 = 1.4 \times 10^{22} s^{-1}$  and  $E_2 = 30.5 \pm 0.3 kJ mol^{-1}$ ,  $Z_2 = 137 s^{-1}$ . The corresponding enthalpy is  $\Delta H = -9.6 kJ g^{-1}$ . The same quantity for the second hydridation is  $\Delta H = -12.5 kJ mol^{-1}$ .

By decreasing the palladium content in the zeolite (sample II, Fig. 5) no changes in the mechanism of absorption or of the kinetic parameters are found. The

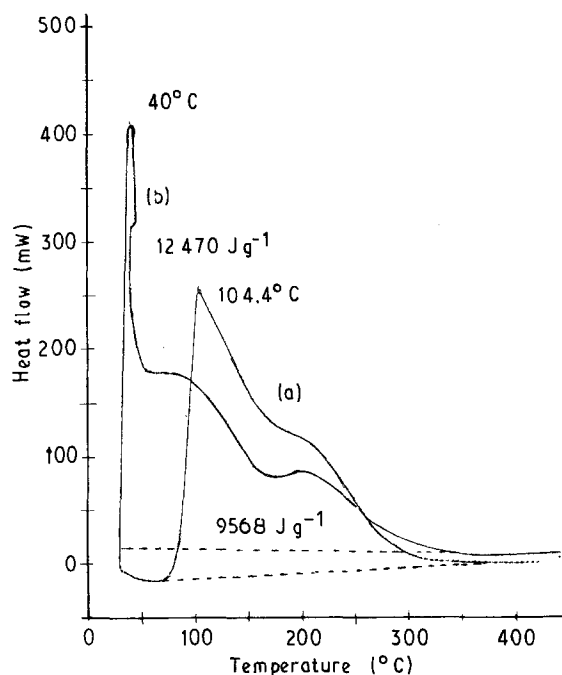


Figure 4 DSC thermograms of zeolite 4A + Pd, sample I: (a) first hydridation, (b) second hydridation after reoxidation for 30 min,  $25 K min^{-1}$ .

enthalpies of the first and second hydridation are  $-10.5$  and  $-18.4 kJ g^{-1}$ , respectively.

It should be pointed out that the kinetic and thermodynamic data obtained for all three investigated systems are valid, according to Equation 1, only for the first process of hydridation.

A summary of the derived kinetic and thermodynamic data is given in Table I.

### 3.2. Thermogravimetric measurements

In the previously described DSC measurements a complex behaviour of the samples on repeated treatment with hydrogen was noticeable. Additional TGA measurements were therefore performed under identical conditions of hydrogen flow.

#### 3.2.1. The $Al_2O_3 + 0.6\% Pd$ system

The correlation of TGA and DSC thermograms shows that at hydridation, at the first instant of hydrogen contact with the sample, a relatively small increase and after that a fast decrease in the weight in a very narrow temperature range is taking place (Fig. 6), followed by a noticeable discharge of water: We believe that the weight increase occurs from the formation of minute amounts of water in the reaction of the absorbed hydrogen and the oxygen which (perhaps) originates from the absorbed air oxygen. This process is catalysed by the palladium present. However, the true process producing the abrupt increase of the exo-peak in curve (a) of Fig. 1 and the sharp decrease in the narrow temperature range in the TGA thermogram is followed by a visible water condensation on the colder parts of the TGA tube. This water originates from the violent reaction of the absorbed hydrogen with the oxygen of the sample itself. Local overheating takes place and the water formed is being liberated before the actual programmed temperature of  $100^\circ C$  is reached in the TGA tube. After the termination of this process, a continuous increase of weight takes place which corresponds to the decreasing part of the exo-peak of the DSC thermogram, which was named the second stage. However, the first hydridation of the sample changes its absorption activity considerably. The hydrided sample, cooled to room temperature in a hydrogen atmosphere and held in air for 30 min or more, loses hydrogen on reaction with oxygen.

On repeating hydridation of the same sample in hydrogen flow, a violent reaction takes place even at room temperature, as shown in the DSC thermogram in curve (b) of Fig. 1 and the TGA thermogram in curve (a) of Fig. 7. Within a few degrees (2 to  $5^\circ C$ ) generation but not evaporation of water occurs, meaning a weight gain. The weight decreases at higher temperature because of the reaction of hydrogen with the oxygen on the sample and local overheating. This corresponds to the loops noticeable in the DSC thermograms. After passing a minimum the weight increases sharply because of the absorption of hydrogen in the overheated sample in the  $70$  to  $80^\circ C$  temperature range. It terminates at about  $300^\circ C$ , in accordance with curve (b) of Fig. 1. The same behaviour is

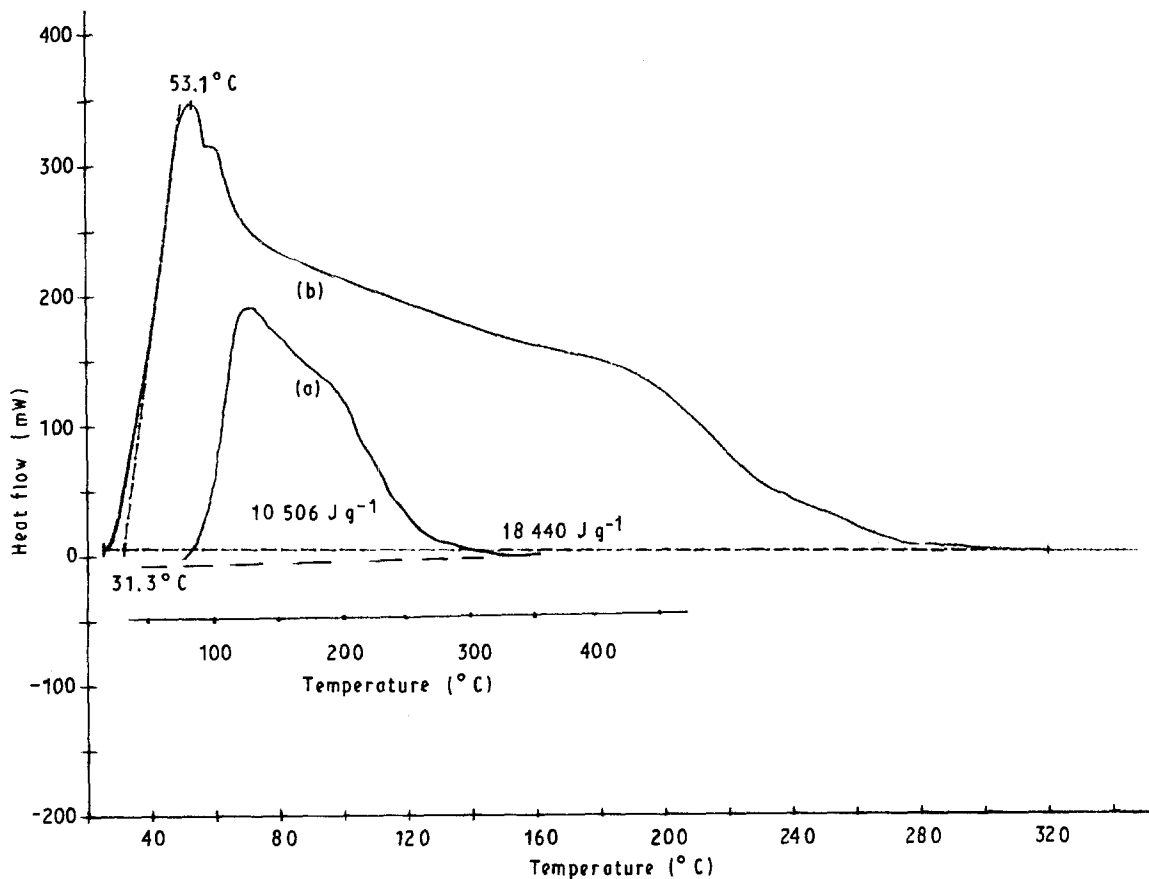


Figure 5 DSC thermograms of zeolite 4A + Pd, sample II: (a) first hydridation, (b) second hydridation after reoxidation, 30 K min<sup>-1</sup>.

TABLE I Kinetic and thermodynamic parameters of the hydridation process

Palladized substances	$E_1(\text{kJ mol}^{-1})$	$E_2(\text{kJ mol}^{-1})$	$Z_1(\text{s}^{-1})$	$Z_2(\text{s}^{-1})$	$-\Delta H'(\text{kJ g}^{-1})$	$-\Delta H''(\text{kJ g}^{-1})$
Al <sub>2</sub> O <sub>3</sub>	120 ± 20	19.8 ± 0.2	$(6.2 \pm 1.1) \times 10^{15}$	33 ± 1.5	11.4	14.4
Y <sub>2</sub> O <sub>3</sub>	157 ± 25	24.4 ± 0.3	$(9.5 \pm 1.6) \times 10^{19}$	130 ± 6	8.1	13.8
Zeolite 4A						
(I)	167 ± 28	30.5 ± 0.3	$(1.4 \pm 0.2) \times 10^{22}$	137 ± 6	9.6	12.5
(II)					10.5	18.4

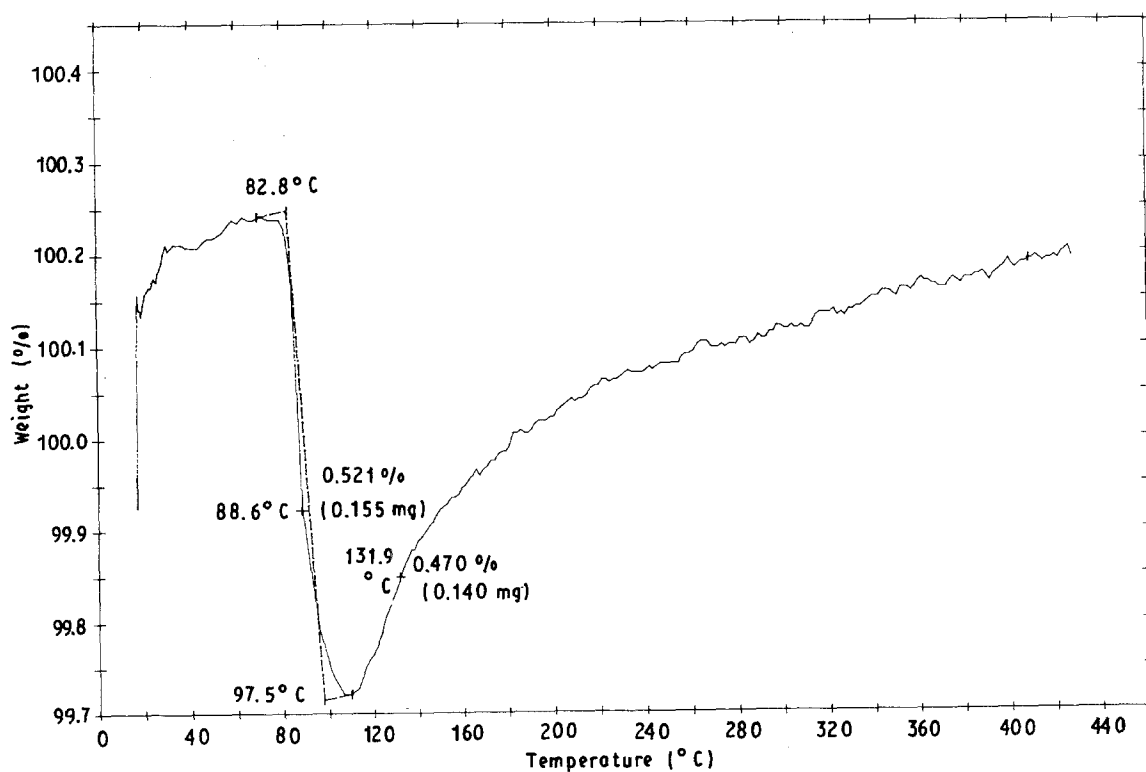


Figure 6 TGA diagram of Al<sub>2</sub>O<sub>3</sub> + 0.6% Pd: first hydridation in hydrogen flow, 30 K min<sup>-1</sup>.

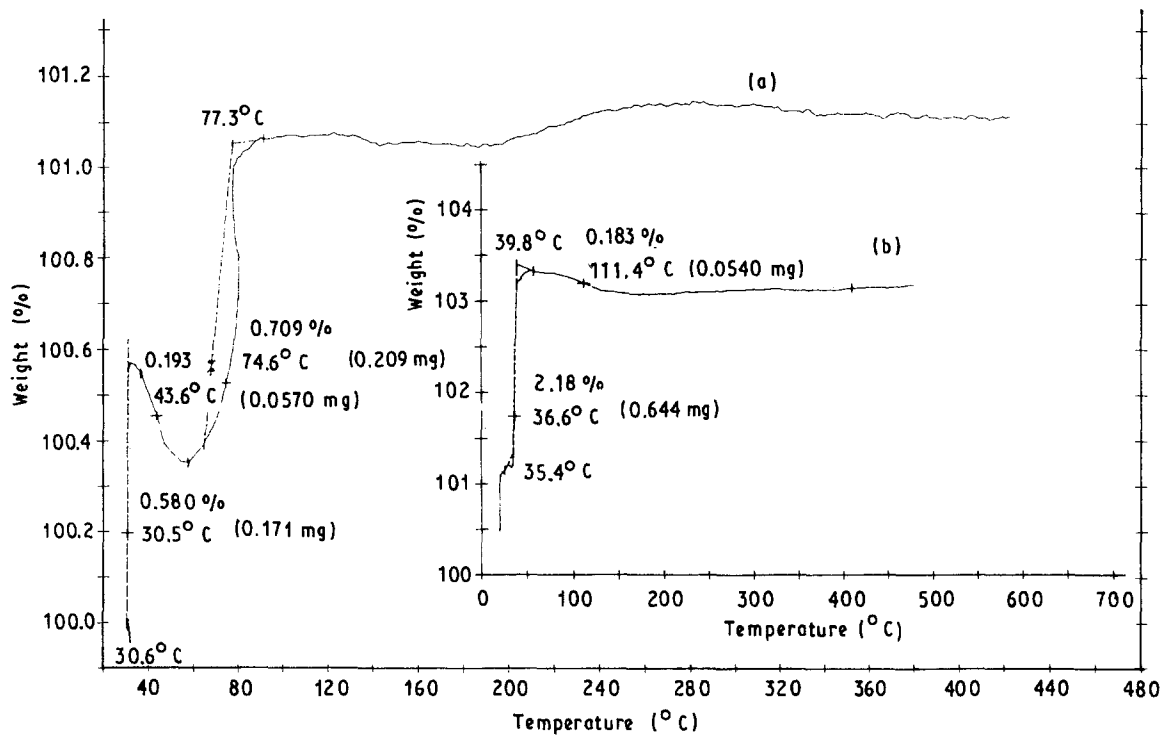


Figure 7 TGA diagram of the second hydridation,  $30 \text{ K min}^{-1}$ : (a)  $\text{Al}_2\text{O}_3 + \text{Pd}$  and (b)  $\text{Al}_2\text{O}_3 + 0.14\% \text{ Pd} + \text{Al}_2\text{O}_3$ , after first hydridation and cooling in hydrogen and exposure to air for several hours.

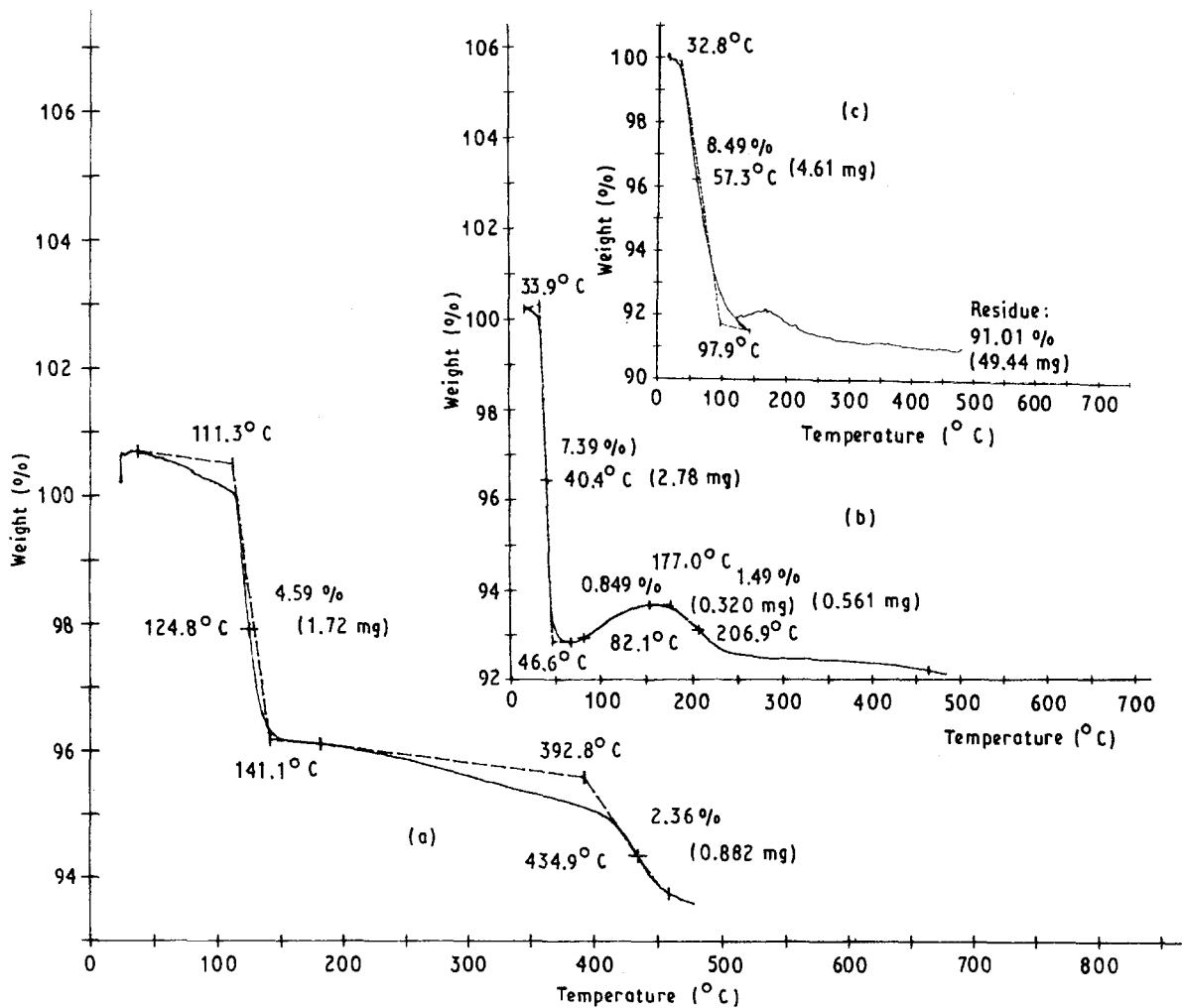


Figure 8 TGA diagrams of  $\text{Y}_2\text{O}_3 + \text{Pd}$ : (a) at first hydridation, (b) second hydridation after cooling in hydrogen and exposure to air overnight, (c) second hydridation of a new sample with increased hydrogen flow and pressure,  $30 \text{ K min}^{-1}$ .

seen with the "diluted" alumina + Pd sample as seen in curve (b) of Fig. 7.

### 3.2.2. The $Y_2O_3 + Pd$ system

On examination by the thermogravimetric method this system behaves similar to palladized alumina. The thermogram in curve (a) of Fig. 8 shows a weight change of the sample at the first hydridation in hydrogen flow. It is seen that in the range between room temperature and 111 °C a small but sudden rise occurs, followed by a moderate decrease because of the evaporation of small quantities of water which was formed in the slow reaction between the absorbed hydrogen and oxygen in the sample, which can be considered as a certain type of preactivation. After that process an abrupt weight loss is recorded accompanied by a visible release of water, which corresponds to the rapid rise of the exo-peak in curve (a) of Fig. 3. Further weight loss (the second stage in the DSC diagram) may be ascribed to a continuation of hydrogen absorption with a decreased rate of water formation up to the end of hydrogen absorption. This is an indication that the  $Y_2O_3 + Pd$  system, like the one involving alumina, undergoes a reduction by formation of water from the absorbed hydrogen and the oxygen of the oxide phase. With both systems a colour change was noticed, most probably due to the amorphization of palladium. At the temperature where the DSC thermogram shows the endothermic minimum

at first hydridation, TGA exhibits a rather steep weight decrease at 435 °C, meaning that the hydride formed loses one of its components (phases), which does not show up in the next hydridation. After hydridation the system loses about 8% of its weight, as seen in Fig. 8. After the first hydridation the sample was left to cool down in a slowly decreasing hydrogen flow, which was stopped when room temperature was reached. Left overnight, atmospheric oxygen penetrated the TGA tube and a considerable quantity of water droplets could be seen on the tube walls. This is obviously a result of reoxidation of the  $Y_2O_3 + Pd$  hydride. During this process the weight of the sample of 35.0 mg after hydridation rose to 37.7 mg, which is practically equal to the original weight of 37.4 mg.

Repeated hydridation of this sample yields the TGA thermogram shown in curve (b) of Fig. 8. The weight loss occurs immediately after the contact with hydrogen in a rather narrow temperature range (34 to 47 °C). This process involves water evolution too, as seen by a condensate on the colder tube walls. Water evaporation takes place at temperatures below the programmed 100 °C because of the overheating of the sample by the violent reaction of the sample and the absorbed hydrogen. However, when this reaction approaches its end, overheating is no longer dominant, water evolution diminishes and the sample weight shows a gain up to the temperature of 150 °C, decreasing later slowly.

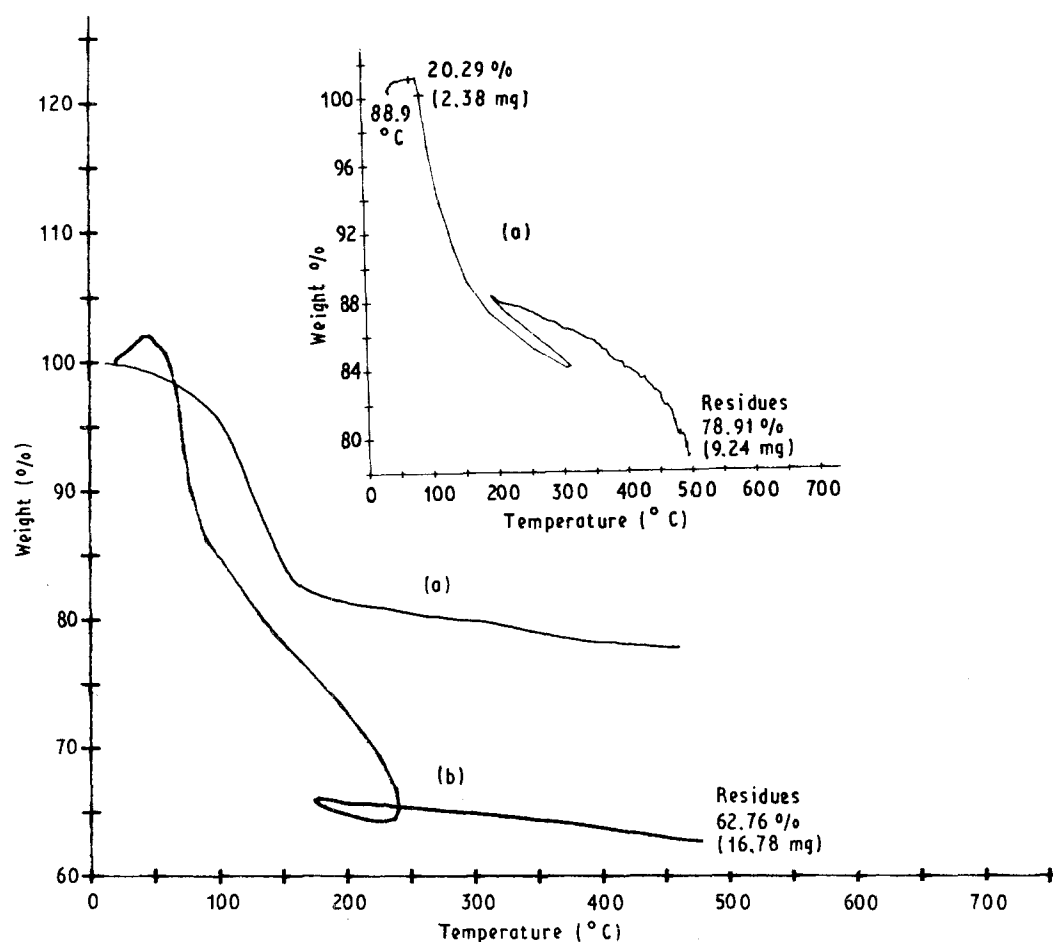


Figure 9 TGA diagrams of zeolite 4A + 0.3% Pd, sample I: (a) first hydridation, (b) second hydridation after contact with air for several hours, 30 K min<sup>-1</sup> (c) first hydridation, increased hydrogen flow.

Curve (c) of Fig. 8 shows the overheating of a sample in an increased hydrogen flow and pressure. Comparison of this thermogram with the DSC thermogram in curve (b) of Fig. 3 shows full agreement in the explanation of the process of hydridation of the  $Y_2O_3 + Pd$  system: namely, the hydride formation is preceded by the process of oxide reduction and water evolution. The hydrides in both the alumina and yttria systems are very reactive towards atmospheric oxygen, the reaction being violent, almost explosive at slightly elevated temperatures. The products of this reaction are water and the reoxidized form of the original substance, which is in turn quite reactive towards hydrogen, even at room temperature.

### 3.2.3. The zeolite 4A + Pd system

Two samples were examined of zeolite with differing palladium contents: the first one (I) with 0.3% Pd and another (II) with 0.025%. At hydridation in hydrogen flow both behave qualitatively like the two oxide systems described above. The process of hydridation (hydrogen sorption) is accompanied by water release and a weight loss in the samples. The hydrided product is a very active absorbent of oxygen, leading to an exothermal formation of water. Curve (a) of Fig. 9 presents a TGA diagram of sample I at first hydridation, showing the weight loss caused by hydrogen absorption which corresponds to the DSC thermogram of curve (a) in Fig. 4, from which the kinetic analysis of the hydrogen absorption was done, but refraining from the explanation of the process of water evolution. By hydridation, as in the case of other oxide systems, the characteristics of the zeolite 4A are being changed to become an active absorbent of hydrogen and of oxygen, if exposed to air for several hours. During this time the sample absorbs oxygen, the hydride is being decomposed releasing water exothermally and the weight of the sample returns to the original value. In this way the sample is prepared for a further hydridation.

Curve (b) of Fig. 9 presents a TGA thermogram showing the effect of overheating because of the violent reaction with hydrogen. The reaction starts from the first contact with hydrogen, showing a slight weight gain. If the flow rate of hydrogen (i.e. its pressure) is increased, hydrogen reacts violently even at the first hydridation, as shown in the thermogram of curve (c). By cycling of the hydridation-dehydridation procedure, the samples are becoming increasingly more active for the reaction with hydrogen and the temperature of absorption is shifted to lower temperatures.

Sample II, with a considerably lower palladium content, behaves in the same way. At the first hydridation the weight of the sample (29.14 mg) increases at the beginning by 0.26 mg because of hydrogen absorption, showing later a clear decrease because of loss of water, as seen in curve (a) of Fig. 10. After the first hydridation the sample was cooled in a hydrogen atmosphere and exposed to air for a longer period of time, thus gaining weight up to 30.85 mg, and hydrided again. Curves (b) and (c) show respectively

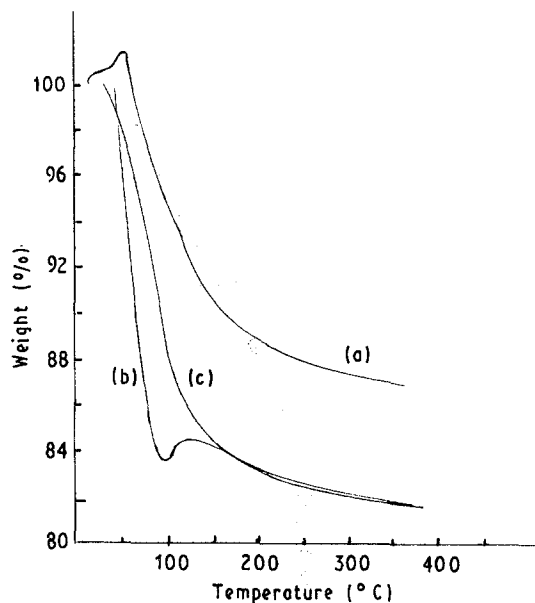


Figure 10 TGA diagrams of zeolite 4A, sample II: (a) first hydridation, (b) 1 second hydridation, (c) spontaneous cooling for several hours in atmosphere of argon containing some oxygen.

the thermograms of the second hydridation and of the spontaneous cooling in an atmosphere of argon which was not completely oxygen-free. A faster weight loss is seen in curve (b) when compared with the first hydridation, since the sample is more active and the chemical reaction heat contributes to the water release. The weight change shows a further slight increase around 100°C which can be explained by additional hydrogen absorption with diminished water evolution. Curve (c) describes the reverse process of slow spontaneous cooling. The weight gain is due to absorption of oxygen present in the argon flow and the recovery of water in the reduced sample. After some 3 h of cooling down to 30°C, the sample reverts to the original weight. This should mean that the processes of sorption and desorption of hydrogen and its reaction with oxygen are reversible. Up to now there was no possibility of analysing the reduced water-free state of samples in order to establish the origin of oxygen in the first hydridation. We believe that in the hydridation process a reduction of the oxide of the solid phase takes place, leading to a non-stoichiometric state which is highly reactive toward both oxygen and hydrogen when reoxidized with atmospheric oxygen.

### 3.3. X-Ray examinations

After the introduction of small quantities of palladium into the investigated oxides and the zeolite, X-ray diffractograms do not show changes in the structure of macro-components. The only change is a weak reflection at about 7° which originates from elemental palladium, but even this vanishes after its amorphization. Hydridation of the palladium-doped oxides and the zeolite does not lead to any noticeable structure change in the samples which are later exposed to air, i.e. reoxidized. Proof of this statement can be found in Figs 11 and 12.



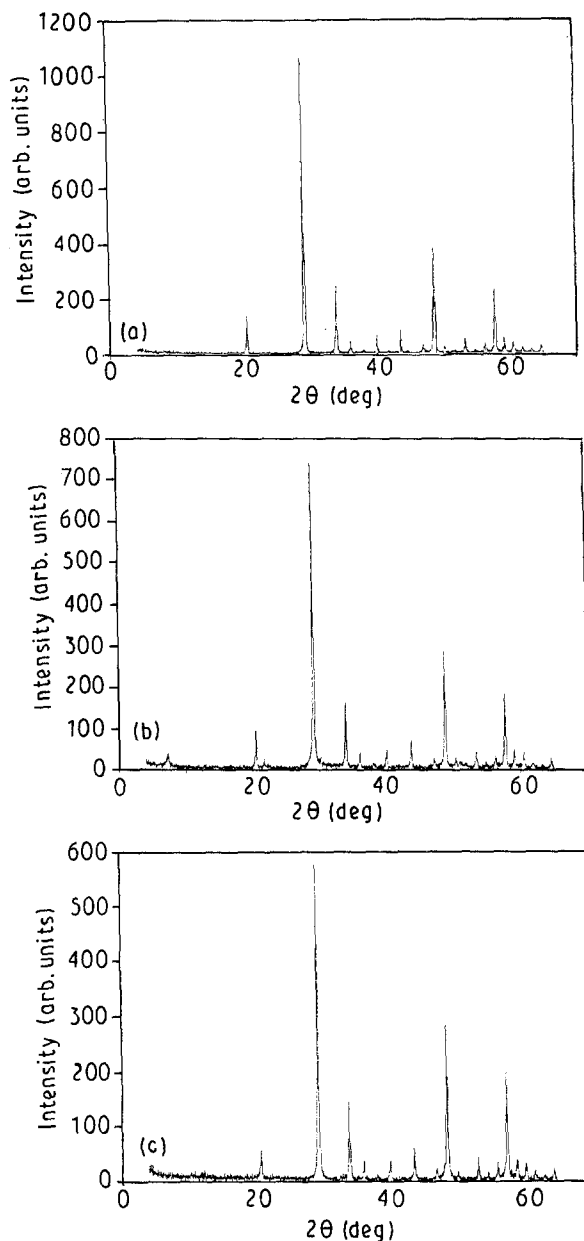


Figure 11 X-ray diffractograms of the  $Y_2O_3 + Pd$  system: (a) standard  $Y_2O_3$ , (b)  $Y_2O_3 + 0.3\% Pd$ , (c) same after hydridation.

#### 4. Conclusions

By introducing small amounts of palladium (0.6 to 0.025%) into the structures of alumina, yttria and zeolite 4A, materials very efficient for hydrogen storage are obtained. Hydridation of these materials in the temperature range between 20 and 450 °C is an exothermal process occurring in two stages. In the first stage an exothermal reaction between hydrogen (spillover hydrogen effect) and the oxygen in the samples takes place, leading to water release and activation of the sample by an almost complete amorphization of the dispersed metallic palladium present. In the second stage hydrogen absorption continues. The product of the initial, first hydridation is very reactive toward oxygen even at temperatures below ambient, while at elevated temperature the reaction is almost explosive, leading to water formation and producing a state which is now very reactive toward hydrogen. The exothermal processes of hydridation and dehydridation (comprising reduction and reoxidation) are re-

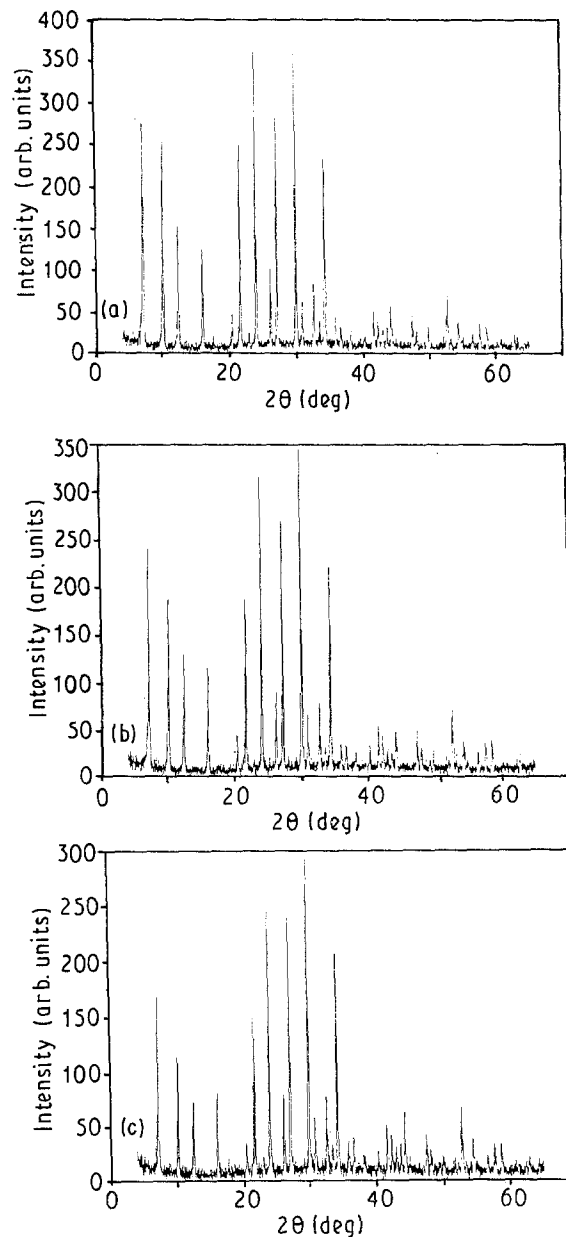


Figure 12 X-ray diffractograms of zeolite 4A + Pd: (a) sample I, (b) same after three hydridations, (c) sample II after three hydridations.

versible without a loss of the base material. The energetic capacities of these materials are quite high and could be used for alternate storage of hydrogen and oxygen and their mutual recombination, leading to water formation and energy release.

Kinetic and thermal parameters of the first process have been determined.

#### Acknowledgement

The author is grateful to Professor S. V. Ribnikar for a number of useful suggestions concerning this work.

#### References

1. P. G. DICKENS, in "Solid State Chemistry of Energy Conversion and Storage", edited by J. B. Goodenough and M. S. Whittingham, Advances in Chemistry Series (American Chemical Society, Washington, DC, 1977) pp. 165-178.
2. P. G. DICKENS, J. H. MOORE and D. J. NEILD, *J. Solid State Chem.* **7** (1973) 241.

3. P. J. WISEMAN and P. G. DICKENS, *ibid.* **6** (1973) 374.
4. M. V. ŠUŠIĆ and Yú. M. SOLONIN, *J. Mater. Sci.* **23** (1988) 267.
5. B. GERARD, G. NOWOGROCKI and J. GUENOT, *J. Solid State Chem.* **29** (1979) 429.
6. B. GERARD, G. NOWOGROCKI and M. FIGLARZ, *ibid.* **38** (1981) 312.
7. P. A. SERMON and G. C. BOND, *JCS Faraday I* **72** (1976) 730.
8. *Idem.*, *ibid.* **76** (1980) 889.
9. M. V. ŠUŠIĆ and Yú. M. SOLONIN, *J. Mater. Sci.* **24** (1989) 3691.
10. H. J. BORCHARDT and D. FARRINGTON, *J. Amer. Chem. Soc.* **79** (1957) 41.

*Received 12 March  
and accepted 1 July 1991*